International Journal of Nanomedicine

Dovepress
Taylor & Francis Group

Open Access Full Text Article

ORIGINAL RESEARCH

Gallic Acid Nanocrystal Hydrogel: A Novel Strategy for Promoting Wound Healing and Inhibiting Scar Formation

Mengtong Yan[1–3,*], Sier Huang[1–3], Xin Li[1–3], Ying Wang[1–3,*], Shuyi Zhong[4], Junfeng Ban[1–4], Shu Zhang[1–3]

[1]Guangdong Provincial Key Laboratory of Advanced Drug Delivery Systems, Guangdong Pharmaceutical University, Guangzhou, People's Republic of China; [2]Center for Drug Research and Development, Guangdong Pharmaceutical University, Guangzhou, People's Republic of China; [3]Guangdong Engineering & Technology Research Center of Topic Precise Drug Delivery System, Guangdong Pharmaceutical University, Guangzhou, People's Republic of China; [4]The Innovation Team for Integrating Pharmacy with Entrepreneurship, Guangdong Pharmaceutical University, Guangzhou, People's Republic of China

*These authors contributed equally to this work

Correspondence: Junfeng Ban; Shu Zhang, Center for Drug Research and Development, Guangdong Pharmaceutical University, Guangzhou, 510006, People's Republic of China, Tel +86 20 39352309, Email banjunfeng@163.com; zzss_97@163.com

Background: Slow healing of skin wounds is a major health problem affecting millions of people each year, and traditional dressings have limited effectiveness in treating them. Gallic acid has anti-inflammatory, antibacterial and antioxidant properties, and combined with nanotechnology can improve its solubility and provide new directions for wound treatment.

Methods: In this study, Gallic acid nanocrystals (GC-NCs) were prepared by a "top-down" method, and GC-NCs were combined with a polyacrylic acid matrix to form Gallic acid nanocrystal hydrogel (GC-NCs-Gel) by co-gelation. The micromorphology, mechanical properties, adhesion properties and bioactivity of GC-NCs-Gel were tested. Finally, the ability of GC-NCs-Gel to promote wound healing and inhibit scar formation was evaluated in a rat whole skin defect model.

Results: The average particle size of GC-NCs was 348.20 ± 1.42 nm, and GC-NCs-Gel had a honeycomb porous structure with excellent swelling properties (963%), water vapor transmission rate (2400 g/m^2/h), tensile stress (28,000 Pa), and adhesive strength (9.6 kPa). GC-NCs-Gel also demonstrated a sustained and controlled drug release property after 48 h of release, the cumulative release was about 57%, and GC-NCs-Gel reached the highest cumulative permeability of 127.2 μg/cm^2 within 6 h. In vitro experiments showed that the inhibition circle diameter of GC-NCs-Gel was 39.75 ± 0.61 mm for *S. aureus* and 21.52 ± 0.06 mm for *E. coli*. The free radical scavenging efficiency of GC-NCs-Gel reached 77.7% in the DPPH assay and up to 98.6% in ABTS. In vivo experiments showed that GC-NCs-Gel accelerated wound healing by promoting neovascularization, epidermal regeneration and collagen deposition.

Conclusion: In this study, a GC-NCs-Gel with anti-inflammatory, antibacterial as well as antioxidant and wound tissue adhesion was prepared. This multi-functional hydrogel has significant advantages in wound healing, and is expected to provide a new and effective means of wound treatment in the clinic.

Keywords: gallic acid nanocrystal hydrogel, hydrogel, wound healing, scarring inhibition

Introduction

Skin injury and scar formation are common problems in clinical care, especially after trauma, burns and surgery. A wound is an injury that results in the loss of continuity in the skin, tissue, and mucous membranes, with clinical features such as pain, erythema, and edema. Scar is an abnormal product of wound healing. The clinical manifestations are slightly different from normal skin, rough surface, local thickening and hardening. Effective wound management is essential to minimize scar formation, accelerate the healing process and improve patients' quality of life. Conventional monofunctional wound dressings, although capable of protecting wounds to a certain extent, often lack healing-promoting and anti-infective active ingredients and have limitations in terms of functionality and comfort. Therefore, the development of hydrogel delivery systems loaded

Received: 7 January 2025
Accepted: 22 March 2025
Published: 11 April 2025

Graphical Abstract

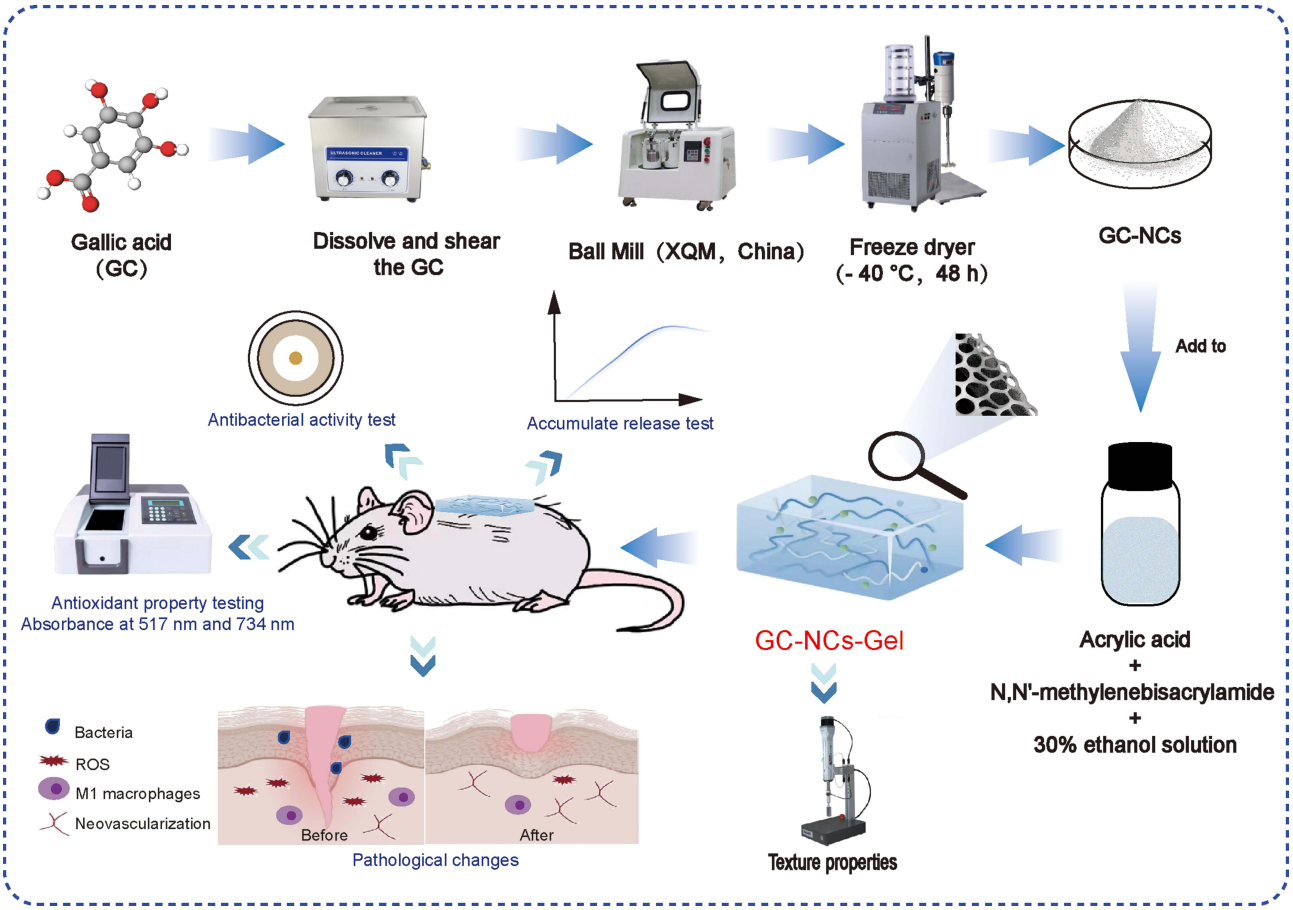

with active ingredients based on the characteristics of wound dressings can not only provide physical protection, but also actively participate in the wound healing process, which has become a hot topic in medical research. In recent years, the application of nanotechnology in drug delivery systems has revolutionized the field of wound therapy. Silver nanoparticles (AgNPs) play an important role in wound healing due to their excellent antibacterial properties.[1] Liu et al prepared tea polyphenol silver nanoparticles (TP@Ag NP) and loaded it into hyaluronic acid hydrogel to obtain HP-TP@Ag NP hydrogel. The hydrogel has significant antioxidant, anti-inflammatory and antibacterial abilities, which can effectively reduce the level of inflammatory factors, and the antibacterial activity against *S. aureus* and *E. coli* was more than 90%, which significantly accelerated wound healing. Liu et al used decellularized extracellular matrix (ECM), GelMA and polydopamine-loaded asiaticoside (AC@PDA) nanoparticles to make a bioactive hydrogel (AC@PDA/ECM-G hydrogel). In the mouse full-thickness excision wound model, this hydrogel group formed a thicker dermis, a higher number of hair follicles regenerated, and a faster wound healing without scar formation than the group without AC@PDA.[2] Nanocrystals refer to the drug particles that are processed to the nanometer level of the drug substance, which can improve the solubility, release and absorption of the drug. Almeleebia et al prepared thymidine and rutin nanocrystals, and loaded them into the gel to obtain thymoquinone + rutin-loaded nanocrystals gel (ThQ + Rut-loaded NC gel). In vivo studies showed that on the 12th day, the wound healing rate of the ThQ + Rut-gel group was 60 ± 13%, and the wound healing rate of the ThQ + Rut-loaded NC gel group was 85.6 ± 7%. The faster wound healing in the ThQ + Rut-loaded NC gel group may be due to the faster solubility and release of nano-sized ThQ + Rut in the gel, which penetrates more into the tissue and accelerates the healing process.[3] Nayak et al prepared a quercetin nanocrystal-loaded hydrogel (Qu-NC Hydrogel), which has slow-release properties, and in vivo studies have

shown that the Qu-NC Hydrogel group promotes wound healing faster compared to the control and the blank hydrogel group.[4] The application of nanoparticles in wound dressings provides a great development prospect for promoting wound healing.

Hydrogel is a polymer system with a three-dimensional network structure containing a large amount of water formed by a simple reaction of one or more monomers.[5,6] It is often used as a medical dressing in wound healing treatment due to its excellent absorbency and solubility, which can be tightly adhered to the wound without adhesion, and can keep the environment moist while absorbing the exudate from the wound.[7,8] Unlike traditional wound dressings such as gauze and bandages, hydrogels do not adhere to the wound or surrounding healthy tissue, thus preventing secondary damage during removal.[9] Hydrogel materials have great potential in scar repair applications due to their high water content, adjustable physical and chemical properties, good compatibility with human body, excellent adhesion to wounds, and similarity to natural extracellular matrix.[10,11] Hydrogels based on polyacrylic acid (PAA) have good hydrophilicity, antimicrobial properties and biocompatibility. Liu et al prepared tea polyphenol/cellulose/silk proteins/polyacrylic acid (SF-OC-PAA-TP) hydrogels showed excellent antimicrobial properties and good biocompatibility in vitro experiments, and in vivo studies have also found that they promote ECM synthesis, angiogenesis, collagen and re-epithelialization and accelerate wound healing.[12] In wound healing, PAA exerts antimicrobial effects and promotes collagen deposition, granulation tissue formation, and neovascularization, and PAA hydrogels have good prospects for application in promoting wound healing.[13]

Gallic acid (GC), a plant polyphenol with antioxidant, anti-inflammatory, and antimicrobial properties, has been extensively studied and used in a variety of therapeutic areas for a wide range of diseases due to its wide range of pharmacological effects. GC is a functional phytochemical that reduces inflammation and oxidative stress.[14] Previous studies have shown that GC has a strong antibacterial effect on gram-positive bacteria and gram-negative bacteria, and the higher the concentration of GC, the more obvious the antibacterial effect.[15] Yang et al found GC accelerated cell migration of keratinocytes and fibroblasts in both normal and hyperglucidic conditions, and may be a potential therapeutic agent for treating wound healing.[16] The use of gallic acid is limited due to its poor pharmacokinetic properties (low absorption, low bioavailability, high metabolism, and low clearance rate).[17] It can be considered that the nanocrystallization of GC and its application in wound dressings can better exert the therapeutic effect of GC. Kaparekar et al prepared gallic acid-loaded chitosan nanoparticles (GA-CSNPs) by ionic gel method and loaded them into collagen fiber scaffolds. An in vivo rat total skin excision model was constructed and the results showed that the GA-CSNPs nanocomposite scaffold group took only 16 days to heal the rat wounds, whereas the collagen fibre scaffold group and the sterile gauze-treated control group took longer to heal the wounds. It is indicated that gallic acid promotes wound healing, and the nanocomposite scaffold is expected to become a new wound dressing for wound healing.[18] Gong et al formed GL hydrogel spontaneously by crosslinking gallic acid (GA) and lysozyme (GL) through fibers. In the *E. coli* infected wound model, compared with the model group, the wound in the GL hydrogel group was almost completely healed on the 9th day, while the wound in the model group was still open, indicating that the GL hydrogel could effectively promote wound healing.[19]

In this study, we innovatively prepared a novel nanogel, GC-NCs-Gel, by homogeneously dispersing gallic acid nanocrystals (GC-NCs) in a polyacrylic acid hydrogel matrix, with the aim of exploring its application in promoting wound healing and inhibiting scar formation. The physicochemical properties, drug release behavior, in vitro antimicrobial and antioxidant efficiencies, as well as the biocompatibility and wound healing effects of GC-NCs-Gel were assessed in a rat skin defect model. Through a series of experiments, we aimed to demonstrate the potential of GC-NCs-Gel as a novel transdermal drug delivery system to improve wound healing efficiency and reduce scar formation, providing a more effective and innovative wound treatment option for clinical use.

Materials and Methods

Materials

N,N′-methylenebisacrylamide, gallic acid, ammonium persulfate and acrylic acid were purchased from Macklin Biochemical Co., Ltd. (Shanghai, China). PVP K30 was purchased from Qingdao Ruiyi Chemical Co., Ltd (Qingdao, China). Sodium dodecyl sulfate and collagenase type II were purchased from Beijing Soleibao Technology Co., Ltd (Beijing, China). 4% paraformaldehyde was purchased from Shandong White Shark Biotechnology Co., Ltd (Shandong, China). Masson staining kit, eosin staining solution, hematoxylin staining solution, Rat TNF-α Elisa Kit, Rat Arg-1 Elisa

Kit, Rabbit Anti-VEGF antibody were purchased from Wuhan Sevier Biotechnology Co., Ltd (Wuhan, China). LB broth medium was purchased from Shanghai Biyuntian Biotechnology Co., Ltd (Shanghai, China). Gram-positive bacteria Staphylococcus aureus and Gram-negative bacteria Escherichia coli were purchased from Beijing Solebold Technology Co., Ltd (Beijing, China).

Preparation of GC-NCs-Gel

In the preliminary stage of the study, we firstly carried out the effect of different stabilizers such as polymers (HPMC K15, HPMC K30, HPMC E30, HPMC E5), non-ionic surfactants (P188, Tween 60, Tween 80), polyvinyl ketones (PVP K30, PVP K90), and HP-β-CD, and SDS on the solubility of GC evaluated. The results showed that the polyvinyl ketone PVP K30 and SDS were more effective than other similar stabilizers in improving GC solubility. Based sodium dodecyl sulphate on this, the process of preparation of gallic acid nanocrystals was carried out using SDS as charge stabilizer and PVP K30 as space stabilizer. The specific preparation method was as follows: firstly, PVP K30 (0.5%) and SDS (0.5%) were accurately weighed according to the prescribed amounts, added to pure water and sonicated by an ultrasonic cleaner (ultrasonic frequency of 53 kHz, ultrasonic power of 100 W) to dissolve them completely and form a stable drug-containing solution. 5% gallic acid was added to the above stabilizer solution. The mixture was subjected to shear treatment for 2 min using a high speed disperser (4000 rpm) to ensure homogeneous dispersion of drug and stabilizer. The drug-containing suspension was transferred to a grinding cup in a ball mill (XQM, China) (ball mill speed 800 rpm for 4 h), which had been pre-filled with zirconium oxide beads (1 mm and 3 mm zirconium oxide beads in a ratio of 1:3) as a grinding medium, and milled for processing. After the grinding was completed, the material was removed and made into powder (GC-NCs) by freeze-drying technique (pre-frozen at −20 °C refrigerator for 24 h, then freeze-dried at −40 °C for 48 h in a freeze-dryer).[20] GC-NCs-Gel was prepared by adding the above nanocrystals to 0.015 g of N,N′-methylenebisacrylamide 30% ethanol solution, and then adding 3 g of acrylic acid, and heating in a water bath at 60 °C for 1 h, to obtain a hydrogel matrix, adding 0.3 g of ammonium persulphate, and heating in a water bath at 60 °C, and gelling that is obtained.[21]

Characterization and Evaluation of GC-NCs-Gel

Morphological Features

The morphology of GC, GC-NCs, Gel and GC-NCs-Gel were analyzed by SEM to observe the different morphologies. Before observation, the samples were pre-treated, appropriate amount of GC and GC-NCs were taken, diluted with purified water, dispersed by ultrasonication (53 Hz, 10 min), a small amount of samples were taken to dry naturally and then sprayed with gold, and the Gel and GC-NCs-Gel were cut into appropriate sizes and placed on conductive adhesive to reveal the cross-section, and the surfaces were sprayed with gold, and placed under the scanning microscope to be photographed.[22]

Water Vapor Transmission Rate (WVTR)

WVTR is an important factor that affects the exchange of water between the skin and the external environment.[21] The experimental temperatures were selected as 37 °C, and the glass bottles were filled with 10 mL of deionized water, after which the mouths of the bottles were covered with Gel, GC-NCs-Gel, and weighed. Saturated ammonium sulphate solution was added at the bottom of the desiccator, and then the glass bottle was put into the desiccator, and the desiccator was placed in a constant-temperature and humidity chamber for 48 h. Finally, the glass bottle was weighed.[23] The WVTR was calculated as follows:

$$WVTR = (W_O - W_T)/\left(10^{-6} \times A \times T\right) \quad (1)$$

Where W_O is the initial weight of the glass bottle and water, W_T is the weight after 48 h, A is the area of the bottle mouth, and T is the time.

Mechanical and Adhesive Properties of GC-NCs-Gel

The tensile properties of hydrogels were tested at room temperature using a texture apparatus.[24] The Gel, GC-NCs-Gel was cut into a rectangular shape with a length of 5 cm, a width of 2 cm, and a thickness of 1 cm. The hydrogel was fixed at both ends of the mass spectrometer and stretched at a speed of 3.33 mm/sec with an inductive element weight of 5 kg. The tensile test was completed when the hydrogel broke from the middle.

The adhesion properties of the hydrogels were carried out at room temperature, and the adhesion properties of the gels were tested using a mass spectrometer. The Gel, GC-NCs-Gel was cut into a rectangular shape with a length of 5 cm, a width of 2 cm, and a thickness of 1 cm. The abdominal skin of an adult Bama pig (The Guangdong Provincial Experimental Animal Monitoring Institute provides Bama pig skin, and its use adheres to animal ethics.) was chosen as the test material, and the hydrogel was adhered between a pair of pig skins, and then the test was carried out by the mass tester with a loading force of 10 N and a tensile speed of 3.33 mm/sec, and the test ended when the hydrogel fell from one side of the pig skin.[25]

Swelling Properties and Degradation Properties

Good swelling and degradation properties are important characteristics to ensure that hydrogels can effectively absorb wound exudate and degrade in vivo, and the swelling and degradation properties of hydrogels were assessed using a weighing method.[26] Gel and GC-NCs-Gel were cut into 3 cm × 1 cm × 0.3 cm to carry out swelling experiments at room temperature. The hydrogel samples were fully immersed in deionized water, and weighed at intervals. Before each weighing, the excess water on the surface of the hydrogel was wiped off, and the weighing data were accurately recorded.[27] After the test, the hydrogel was dried and weighed, and the swelling rate of the hydrogel was calculated according to the following formula:

$$Q(\%) = \frac{W_i - W_O}{W_O} \times 100\% \tag{2}$$

Where Q is the swelling rate of the hydrogel, W_i is the mass of the swelling hydrogel, and W_O is the original mass of the hydrogel.

The Gel and GC-NCs-Gel were cut into 3 cm × 1 cm × 0.3 cm size. The initial mass M_0 of the hydrogel before drying was recorded first; then, hydrogels of the same size mass were placed in type II collagenase solution, and the hydrogels were removed at 20 h, 40 h, 60 h, 80 h, and 100 h. The hydrogels were rinsed, followed by freeze-drying and weighing, which was recorded as M_1, with three samples in parallel for each group.[28] The formula was calculated as follows:

$$D(\%) = \frac{M_0 - M_1}{M_0} \times 100\% \tag{3}$$

Where D is the degradation rate of hydrogel, M_1 is the mass of degraded hydrogel, and M_0 is the original mass of hydrogel.

Spectroscopic Analysis of GC-NCs-Gel

The crystal structures and phase compositions of GC, GC-NCs, Gel and GC-NCs-Gel were analyzed by X-ray diffractometry, and the diffraction peaks of the drug crystals were determined to reveal whether there are any structural differences between GC and GC-NCs.[29] Measurement conditions: Cu target, working conditions of tube voltage 40 kV, tube current 40 mA, scanning range 0–40°, scanning speed 4°/min. For the XRD characterization of Gel and GC-NCs-Gel, it was revealed whether there was any change in the crystalline shape of the GC-NCs loaded into the hydrogel. The gels were cut to the size of 20 mm × 20 mm and placed on aluminum sheets for testing, and the gels were flattened on slides for testing. The scattering angle (2θ) was from 5° to 90° and the scanning speed was 4°/min.

The characteristic absorption peaks of GC and GC-NCs were analyzed by FT-IR spectrophotometer, and GC and GC-NCs were mixed with appropriate amount of KBr and ground into powder, and pressed into a transparent thin film for analysis in the wavelength range of 4000–500 cm^{-1}. GC and GC-NCs were compared to illustrate whether there was any change in the structure of GC after GC was prepared into nanocrystals; in order to further understand whether there was any structural change after GC- NCs were loaded into hydrogels to see if the structure changed, Gel and GC-NCs-Gel were also analyzed for absorption wavelengths.[30]

GC, GC-NCs, Gel and GC-NCs-Gel were thermally analyzed using a differential scanning calorimeter to observe the absorption (exothermic) peaks.[31] The DSC peaks were analyzed to determine whether there was any change in the crystalline shape of the nanocrystals after GC was prepared into them. DSC analysis of Gel and GC-NCs-Gel was performed to show whether there was any change in the crystalline shape of nanocrystals after GC-NCs were loaded into the hydrogel. The GC, GC-

NCs, Gel and GC-NCs-Gel were placed in an aluminum crucible and pressed tightly in a DSC bath under the working conditions of nitrogen flow rate of 20 mL/min, and the temperature was increased from 28 °C to 300 °C at a rate of 10 °C/min. The measured results were plotted into a DSC curve.

In Vitro Release and Transdermal Study

In vitro release was evaluated according to previously reported methods.[32] The 2 g GC-NCs-Gel was dissolved in 10 mL normal saline and placed in a thermostatic oscillator at 37 °C and 100 rpm/min. Sampling points were set at 2, 4, 6, 8, 10, 12, 24 and 48 h. 1 mL of solution was taken each time, and an equal amount of saline was supplemented after sampling to maintain the volume. The resulting solution was filtered and the content was determined by HPLC, the cumulative release rate was calculated, and the in vitro release curve of GC-NCs-Gel was plotted.

$$Q_n = \frac{\mathrm{V}C_n + \sum_{i=1}^{n-1} C_i V_i}{\mathrm{m}} \times 100\% \tag{4}$$

Where Q_n is the cumulative release percentage of the drug, V is the volume of the release medium, C_n is the drug concentration in the release medium at the nth sampling, C_i is the drug concentration in the release medium at each sampling, V_i is the volume of each sampling, and m is the total amount of the drug.

In vitro transdermal experiments of GC-NCs-Gel were performed using Franz transdermal diffusion.[33] Prior to the experiment, the skin on the back of SD rats was clipped and subcutaneous fat and connective tissue were removed. Saline was used as the receiving solution, and the skin was fixed in the Franz transdermal diffusion apparatus. After checking that there was no leakage, the receiving solution was filled and the air bubbles were eliminated, and the GC-NCs-Gel was cut into a size suitable for the supply pool, applied to the skin surface, and sealed with parafilm. At 2, 4, 6, 10, 14, 16, and 24 h, 1 mL of receiving solution was withdrawn, and an equal amount of saline was added. After filtration, the content was determined by HPLC, and the cumulative permeation amount per unit area (Q_n) was calculated.

$$Q_n = (C_n V_s + \sum_{i=1}^{n-1} C_i V)/S \tag{5}$$

Where C_n is the concentration of GC-NCs in the permeate at the nth time point, C_i is the concentration of GC-NCs in the permeate at the ith time point, V_s is the volume of the receiving cell, V is the sampling volume of the receiving liquid, S is the effective penetration area of the diffusion cell.

In Vitro Antibacterial and Antioxidant Assay

Escherichia coli (*E. coli*) and Staphylococcus aureus (*S. aureus*) were used as model strains for the experiments, and all the manipulations were done on an ultra-clean bench.[34] Single colonies of these two bacteria were removed from LB solid medium (Peptone, sodium chloride, glucose, yeast paste powder) and inoculated into 5 mL of LB broth medium, and incubated at 37 °C and 180 rpm for 12–16 h until the bacteria entered into the logarithmic growth phase. The bacterial concentration was adjusted to an OD_{600} of 0.6–0.8 using a UV-Vis spectrophotometer, and then stored at 4 °C. The evaluation of antibacterial ability was achieved by measuring the diameter of the inhibition zone. Gel and GC-NCs-Gel were made into a circular gel with a diameter of 6 mm, and the GC solution was adjusted to an appropriate concentration according to the drug loading rate of the hydrogel. The LB solid medium was poured into the culture dish, and 10^8 CFU/mL of *E. coli* and *S. aureus* were inoculated to ensure that the bacteria were evenly distributed. A sterile filter paper with a diameter of φ = 6 mm was placed on the surface of the culture medium using sterile tweezers. The circular gel and 10 μL GC solution were placed on the filter paper, respectively, and the control group was not treated. The culture dish was placed in a constant temperature incubator at 37 °C for 12 h. After the culture, the diameter of the bacteriostatic ring including the filter paper was measured with a vernier caliper, and the data were recorded and photographed. The experiment was repeated three times.[35–38]

In this experiment, the in vitro antioxidant capacity of hydrogels was evaluated by DPPH and ABTS free radical scavenging experiments.[39,40] Firstly, Gel and GC-NCs-Gel were immersed in 2 mL of 0.04 mg/mL DPPH solution, respectively, and the blank DPPH solution was used as a control. After 30 min of dark reaction at room temperature, the absorbance was scanned in the range of 300–800 nm using a spectrophotometer, especially the absorbance at 517 nm. The DPPH free radical scavenging rate was calculated according to Formula (6).

Similarly, in the ABTS experiment, 7.4 mM ABTS and 2.6 mM potassium persulfate were mixed at a ratio of 1:1 for 12 h in the dark, and then Gel and GC-NCs-Gel were mixed with 2 mL ABTS solution. The blank ABTS solution was used as a control, and the reaction was carried out at room temperature for 5 min in the dark. The absorbance at 734 nm was recorded using a spectrophotometer at the same wavelength range, and the ABTS radical scavenging rate was calculated according to formula (7).

$$DPPH\ scavenging\ rate(\%) = \frac{A_0 - A_i}{A_0} \times 100\% \tag{6}$$

Where A_0 are the absorbance value of the control substance, and A_i are the absorbance value of the mixed solution of hydrogel and DPPH.

$$ABTS\ scavenging\ rate(\%) = \frac{A_0 - A_1}{A_0} \times 100\% \tag{7}$$

Where A_0 are the absorbance value of the control substance, and A_1 are the absorbance value of the mixed solution of hydrogel and ABTS.

Excision Wound Healing Study

The rats were ear-marked and anesthetized using isoflurane inhalation. After shaving the backs of the rats, the shaved areas were cleaned with saline, and then two circular skin defects of 1 cm in diameter were created on the back of each rat using a sterile perforator to ensure consistency of the defects to ensure the accuracy and comparability of the experimental results. After that, each wound was inoculated with 50 μL (10^8 CFU/mL) of Staphylococcus aureus and Escherichia coli suspensions, and the wounds were kept exposed and the bedding changed regularly to maintain hygiene. The experimental rats were randomly divided into three groups: blank group, model group and experimental group, of which 18 rats were in each of the model and experimental groups, and 4 rats were in the blank group. The rats in the model group were modeled with skin defects but without GC-NCs-Gel, while the experimental group had GC-NCs-Gel applied to the wounds every two days for 15 consecutive days. The hydrogel was covered over the wound in the form of discs with a diameter of 10 mm and a thickness of 1 mm. It was fixed with gauze and medical tape to prevent infection and mutual tearing between rats. After surgery, skin photographs of rats were taken on days 0, 3, 7, 11, and 15. The wound area was measured by Image J software, and the wound closure rate was calculated. The formula was as follows:

$$Wound\ closure\ rate(\%) = \frac{A_0 - A}{A_0} \times 100\% \tag{8}$$

(where A_0 is the wound area immediately after surgery, and A is the wound area after surgery on days 3, 7, 11 and 15). To investigate the molecular mechanism of hydrogel to inhibit scar formation, rats were sacrificed at the end of the experiment (day 15), and 0.2 cm of skin tissue from the wound edge was excised and fixed in 4% paraformaldehyde. The recovery of skin appendages was assessed by H&E staining, collagen fiber maturation was assessed by Masson staining, anti-inflammatory effect was assessed by TNF-α and Arg-1 immunofluorescence staining, and pro-angiogenic factor expression was detected by VEGF immunohistochemical staining.

Statistical Analysis

The experimental data were expressed as mean ± standard deviation. Pairwise comparisons were made by a two-sample *t* test. One-way ANOVA was used for comparison between multiple groups. The tests revealed no significant differences when $P > 0.05$.

Results and Discussion

Preparation of Nanocrystals Based Gel by Co-Gel Method

The preparation process of nanocrystals requires the treatment of raw drugs to nanoscale drug particles. This process usually requires stabilizers to reduce the aggregation of drug crystals and ensure the stability of the nanocrystalline system.[41,42] In the experiment, we first prepared gallic acid (GC) into nanocrystals (GC-NCs) and loaded them into hydrogels for the study of wound healing. The results showed that PVP K30 and SDS as stabilizers could effectively improve the solubility of GC

(Figure 1A). PVP K30 is adsorbed on the surface of nanocrystals to form a protective film, which maintains the stability of nanocrystals by steric hindrance effect. SDS is an ionic surfactant, which hinders the aggregation of nanocrystals through electrostatic repulsion, thereby maintaining the stability of nanocrystals.[43] Therefore, PVP K30 was selected as the spatial stabilizer and SDS as the charge stabilizer. After preparation into nanocrystals, the average particle size of GC-NCs was 348.20 ± 1.42 nm, and the solubility of GC-NCs was significantly increased (Figure 1B). In addition, we found that GC-NCs-Gel could be

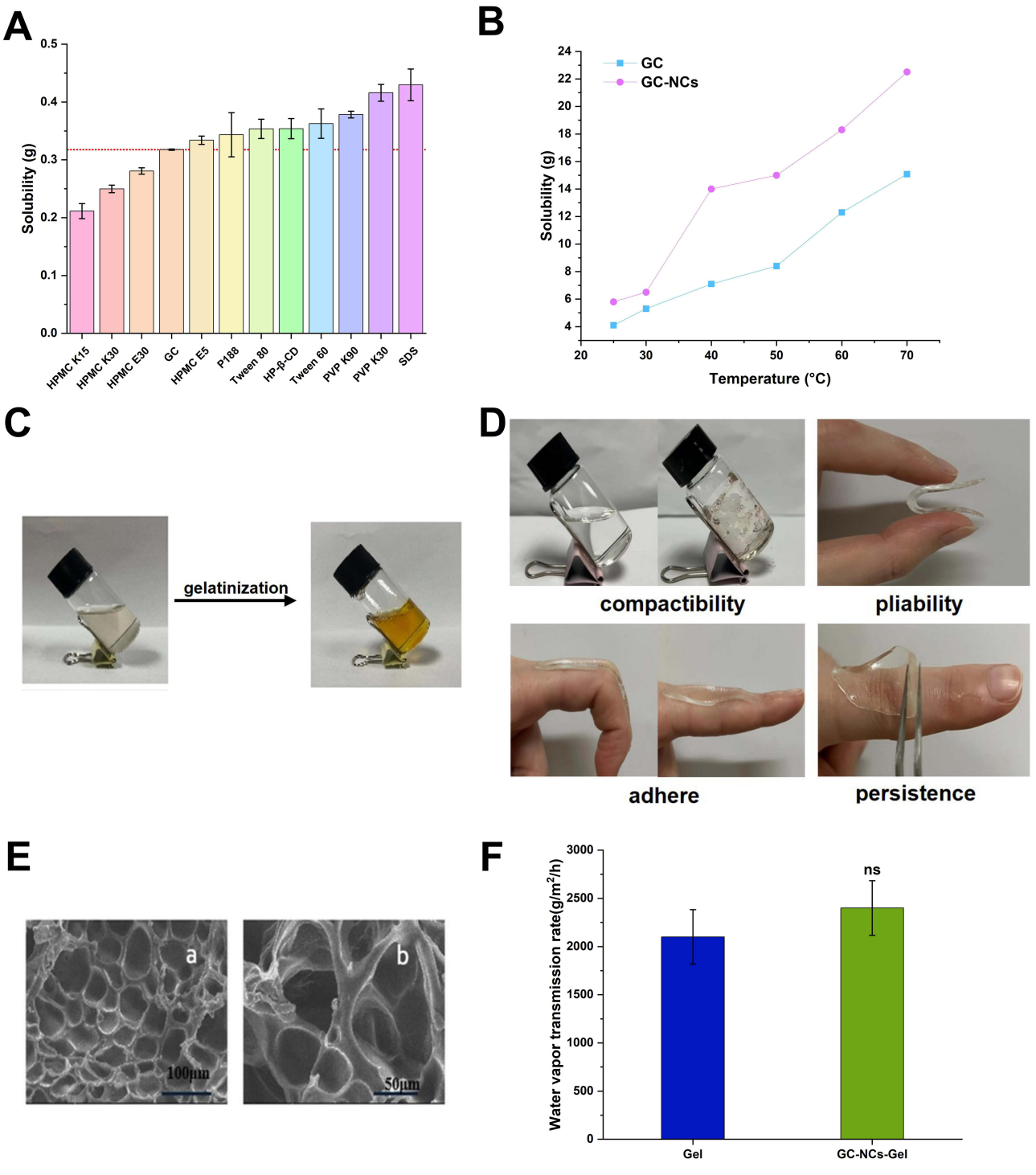

Figure 1 (**A**) Effect of different stabilizers on GC solubility. (The dashed red line represents whether different stabilizers have solubilization effect on GC based on the solubility of GC) (**B**) Comparison of the solubility of GC and GC-NCs. (**C**) Gelation process. (**D**) Evaluation of gel appearance and morphology. (**E**) Scanning electron microscope images of Gel and GC-NCs-Gel (a is Gel, b is GC-NCs-Gel). (**F**) Water vapor transmission rate of Gel and GC-NCs-Gel. ($^{ns}P>0.05$).

formed within 15 min, and this process was related to the interaction between the phenolic hydroxyl group on gallic acid and the amino group on the hydrogel matrix chain, and this mode of action was the main factor for the good formability of the hydrogel (Figure 1C). In evaluating the potential of hydrogels as wound dressings, we observed their formability, flexibility, adhesion, and residual properties. As shown in Figure 1D, Gel demonstrated good formability and exhibited excellent elasticity and flexibility when subjected to external mechanical forces such as bending. In the process of bending the thumb joint from 90° to 0°, Gel can completely fit the skin surface, and does not shift, damage or residue during removal, and is easy to remove. Scanning electron microscopy (SEM) observation (Figure 1E) showed that the Gel preparation had a honeycomb structure, which not only gave GC-NCs-Gel air permeability, but also enabled GC-NCs to be evenly distributed in the gel polymer network. This structure helps to keep the wound moist and promote wound healing. In addition, a good water vapor transmission rate (WVTR) of the hydrogel is essential to maintain the wound moist state. We found that the WVTR of both Gel and GC-NCs-Gel was in the range of 2000–2500 $g/m^2/h$ at 37 °C (Figure 1F), which fulfils the requirement of an ideal hydrogel.[44] The results of the above studies showed that the GC-NCs-Gel prepared by co-gelation method showed excellent performance in terms of formability, flexibility, permeability and water vapor transmission rate, which has the potential for drug delivery.

Properties of GC-NCs-Gel

Ensuring that the hydrogel delivery system has the necessary flexibility, elasticity, and tensile resistance to accommodate the body's movement and daily activities is a primary consideration for research. According to the experimental results (Figure 2A), the tensile stress of the hydrogel increased significantly to 28,000 Pa with the addition of GC-NCs, showing its excellent tensile properties. Adhesion performance is one of the key properties of transdermal delivery systems, which directly affects the stability and durability on the skin. In daily life, wounds may be subjected to bending and squeezing due to various activities. If the adhesion properties of the hydrogel are insufficient, it may shift or fall off under these external forces.[45] The experimental data showed that the adhesion strength of Gel was 4.1 kPa, whereas the adhesion of GC-NCs-Gel to pig skin was significantly enhanced to 9.6 kPa after the addition of GC-NCs (Figure 2B and C). In addition, the long-term adhesion of the hydrogel was tested over a period of 20 days (Figure 2D), and the results showed that the hydrogel was still able to maintain good adhesion to pig skin. The hydrophilicity of the hydrogel is one of its remarkable properties, which allows the gel polymer network to absorb and retain a large amount of water, thus absorbing exudate from the wound tissue.[46] The addition of GC-NCs affects the swelling properties of hydrogels. As shown in Figure 2E, the swelling ratio of GC-NCs-Gel increased with the addition of GC-NCs, and the swelling ratio reached equilibrium at the 40 h. The change in the degree of swelling indicated that the smaller the degree of swelling, the tighter the cross-linking of the internal mesh structure of the gel. Finally, the degradation rate of the hydrogel is another important consideration. As shown in Figure 2F, the addition of GC-NCs significantly accelerated the degradation rate of the gel, which had degraded by about 40% within 60 h, whereas the Gel degraded by only about 20% in the same time. This suggests that Gel is densely cross-linked internally and therefore has a slower degradation rate. In contrast, GC-NCs-Gel reduced the internal cross-link density of the hydrogel due to the incorporation of GC-NCs, which accelerated the degradation of the hydrogel. Through the above experiments, the tensile properties, adhesion properties, swelling properties and degradation rate of the hydrogel materials, which are the key properties of transdermal drug delivery systems for wound healing, were evaluated and optimized. Through these improvements, we were able to provide a more effective and reliable hydrogel drug delivery system for wound healing.

Analysis of Drug Distribution

The X-ray diffraction (XRD) pattern (Figure 3A) revealed characteristic diffraction peaks of gallic acid (GC) in the interval from 15° to 30°, indicating that it exhibits a crystalline state. The positions of the diffraction peaks of the prepared and obtained GC nanocrystals (GC-NCs) did not change significantly in the same angular range as compared to GC, indicating that the preparation process using PVP K30 and SDS as stabilizers did not lead to a significant change in the crystalline form of the GC-NCs. Further, the characteristic diffraction peaks of GC-NCs in the interval from 15° to 30° (Figure 3B) also confirmed their crystalline state, and the characteristic diffraction peaks remained unchanged when they were doped into the hydrogel, which indicated that the crystalline morphology of the GC-NCs in the hydrogel was maintained. Fourier transform infrared spectroscopy (FT-IR) analysis showed that both GC and GC-NCs had absorption peaks of -OH near 3500 cm^{-1} and C=O at 1740 cm^{-1}. The characteristic peaks at 998, 1328, 1560, and 3215 cm^{-1} corresponded to the bulk drug GC, which confirmed that the drug structure remained

 https://doi.org/10.2147/IJN.S514961

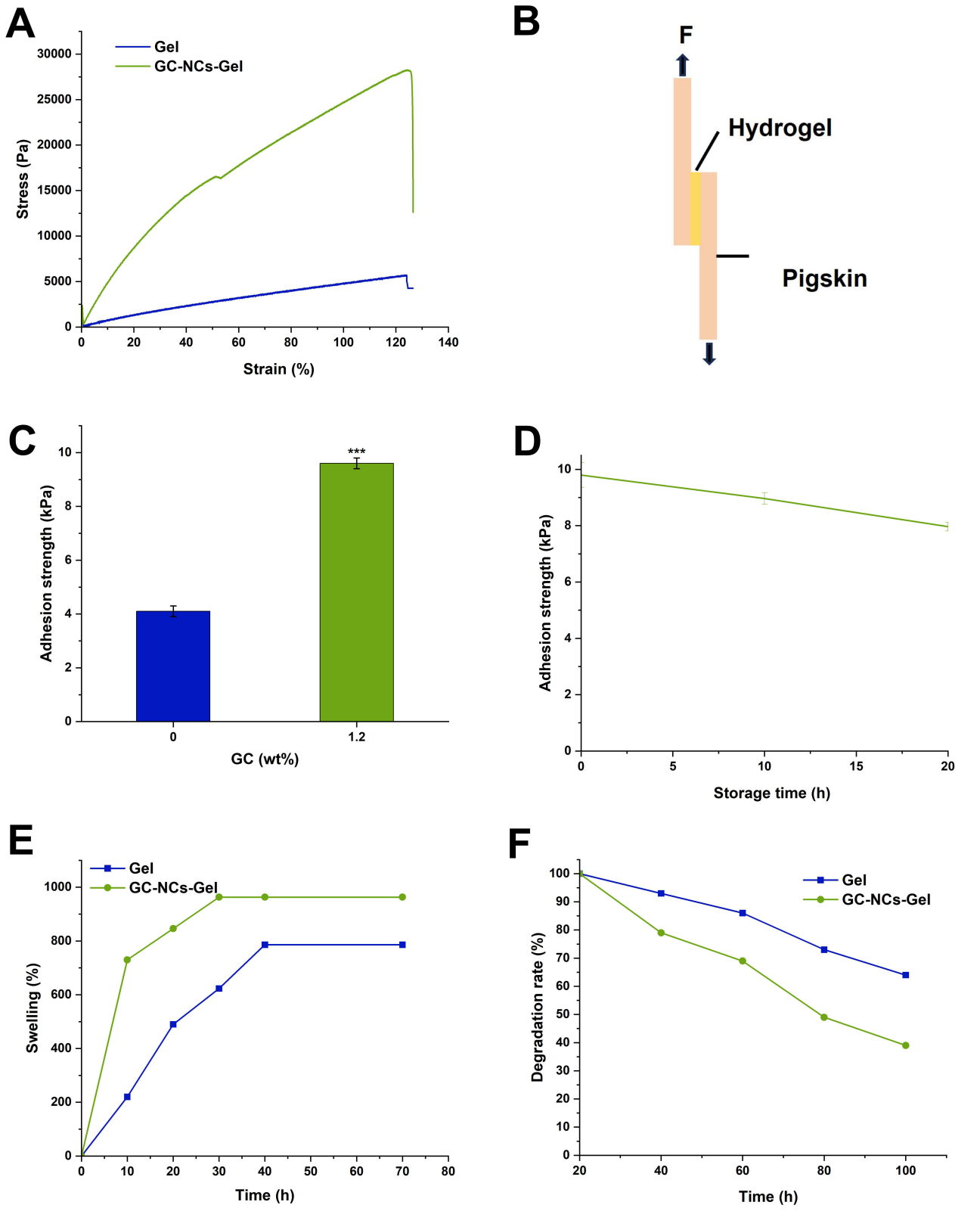

Figure 2 (**A**) Tensile stress-strain curves of Gel, GC-NCs-Gel. (**B**) Schematic diagram of adhesion experiments. (**C**) Hydrogel adhesion strength. (**D**) Hydrogel long-term adhesion. (**E**) Dissolution curves of Gel, GC-NCs-Gel (**F**) Degradation curves of Gel, GC-NCs-Gel. (****P* < *0.001*).

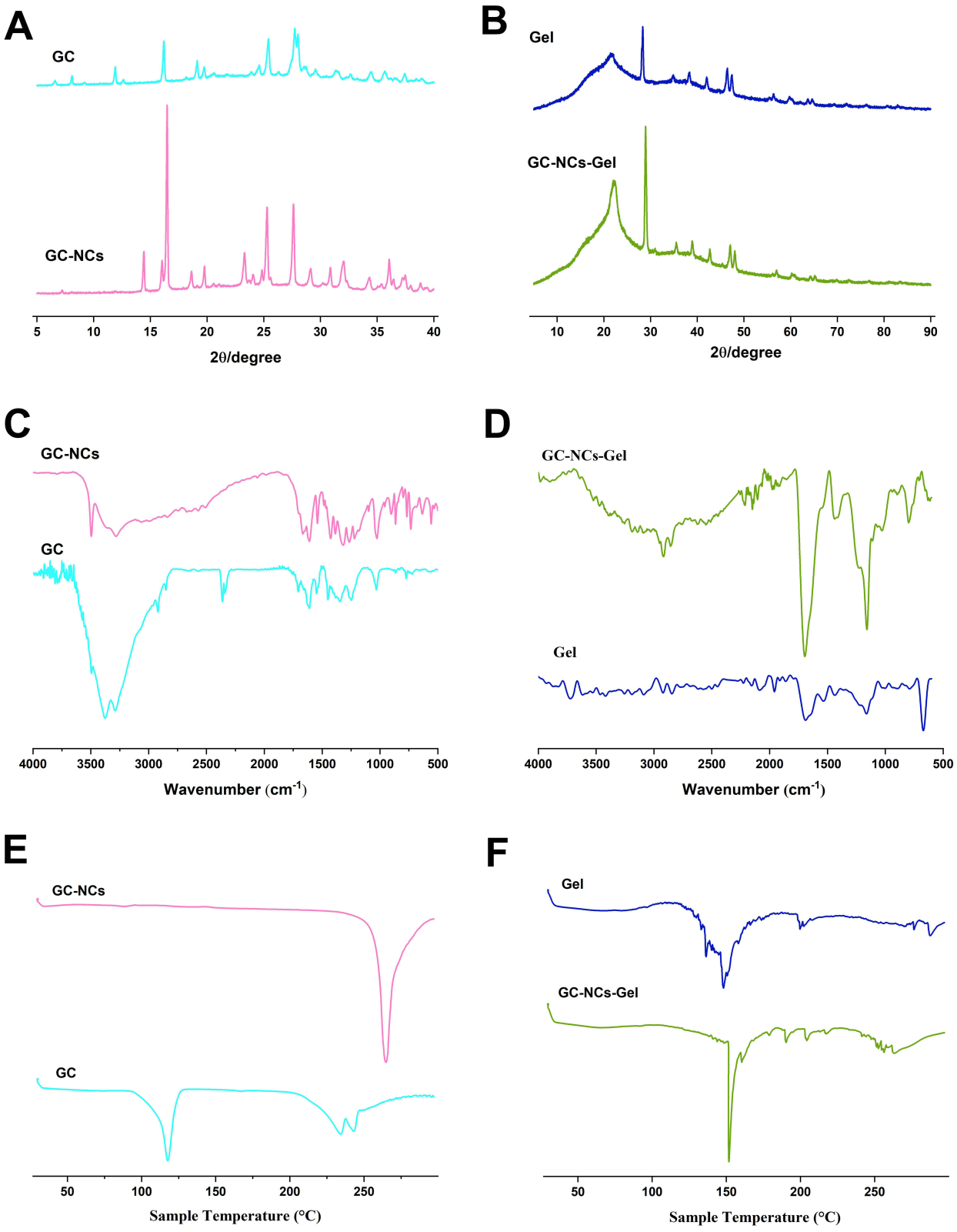

Figure 3 (**A**) X-ray diffraction characterization of GC, GC-NCs. (**B**) X-ray diffraction characterization of Gel, GC-NCs-Gel. (**C**) FT-IR analysis of GC, GC-NCs. (**D**) FT-IR analysis of Gel, GC-NCs-Gel. (**E**) DSC analysis of GC, GC-NCs. (**F**) DSC analysis of Gel, GC-NCs-Gel.

https://doi.org/10.2147/IJN.S514961

essentially unchanged in the prepared GC-NCs, thus validating the feasibility of the preparation method (Figure 3C). Infrared spectral analysis of the hydrogel (Gel) and the hydrogel containing GC-NCs (GC-NCs-Gel) (Figure 3D) showed that there was a C=O absorption peak at 1740 cm^{-1}, the stretching vibration peak of the C=O bond in the carboxyl ion (-COO) of acrylic acid was located at 1407 cm^{-1}, and the characteristic peaks at 998, 1328, 1560, and 3215 cm^{-1} were consistent with the main characteristic peaks of GC-NCs, indicating that the GC-NCs had been uniformly dispersed in the honeycomb pore structure. The characteristic peaks were consistent with the main characteristic peaks of GC-NCs, indicating that the GC-NCs had been uniformly dispersed in the honeycomb pore structure of the hydrogel. The differential scanning calorimetry (DSC) curves (Figure 3E) showed that GC had an endothermic peak at about 130 °C, whereas the endothermic peak of the drug for GC-NCs shifted to the right at about 250 °C, which may be due to the effect of the exothermic peak of the excipients. The experimental results showed that the crystalline form of GC did not change significantly after media milling and still existed in crystal form. From the DSC curves of Gel and GC-NCs (Figure 3F), it can be seen that the absorption peaks shifted to the left after GC-NCs were loaded into the hydrogel mesh structure, which indicated that the GC-NCs loaded into the hydrogel existed in an amorphous form, and the preparation process of the GC-NCs-Gel had no effect on the nanocrystal structure. By means of XRD, FT-IR and DSC analyses, we confirmed the stability of the crystalline form and drug structure of GC-NCs during the preparation process, as well as their homogeneous dispersion in the hydrogel. These results provide a scientific basis for GC-NCs-Gel as a potential transdermal drug delivery system.

In Vitro Drug Release and Transdermal Analysis

The results of in vitro release experiments (Figure 4A) demonstrated that GC-NCs-Gel released the drug rapidly during the initial phase, a phenomenon that helps to achieve the desired minimum effective drug concentration in a shorter period of time, resulting in a rapid drug effect. In addition, GC-NCs-Gel exhibited sustained and controlled drug release characteristics, with a cumulative release of approximately 57% after 48 h of release. This pattern of drug release helps to maintain a stable drug concentration, supporting the achievement of long-term therapeutic effects. As a transdermal delivery system, GC-NCs-Gel needs to have excellent drug transmission rate. Figure 4B shows that GC-NCs-Gel reached the highest cumulative transmittance of 127.2 μg/cm^2 within 6 h. This result confirms that the preparation of GC into nanocrystals has a significantly improved drug transmittance rate, indicating that GC-NCs-Gel has potential clinical applications as an effective transdermal delivery system. The preparation method and drug release characteristics of GC-NCs-Gel have shown good drug delivery potential, which is of great significance for the development of new transdermal drug delivery systems.

In Vitro Antibacterial and Antioxidant Efficiencies of GC-NCs-Gel

In this study, we evaluated the antibacterial activity of GC, Gel and GC-NCs-Gel against *S. aureus* and *E. coli*. The results of the inhibition zone test (Figure 5A) showed that after incubation at 37 °C for 12 h, the GC group only produced a slight inhibition zone against the two bacteria, while GC-NCs-Gel and Gel showed significant antibacterial effects.

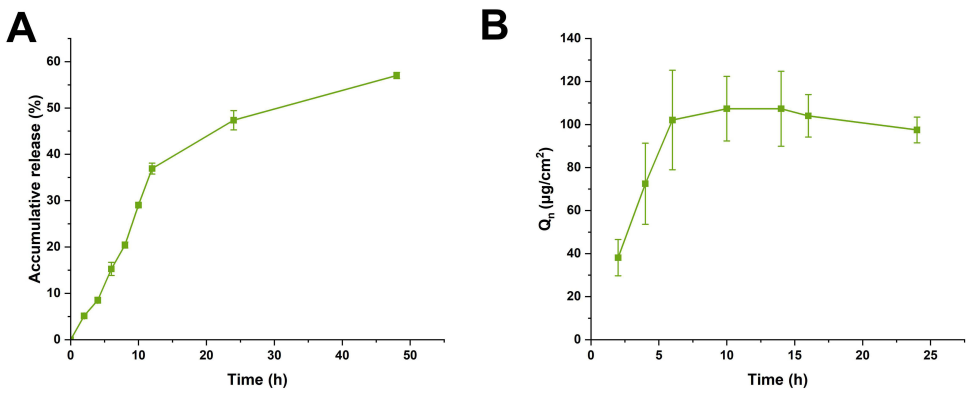

Figure 4 (**A**) In vitro release profile of GC-NCs-Gel. (**B**) Percutaneous drug permeability of GC-NCs-Gel.

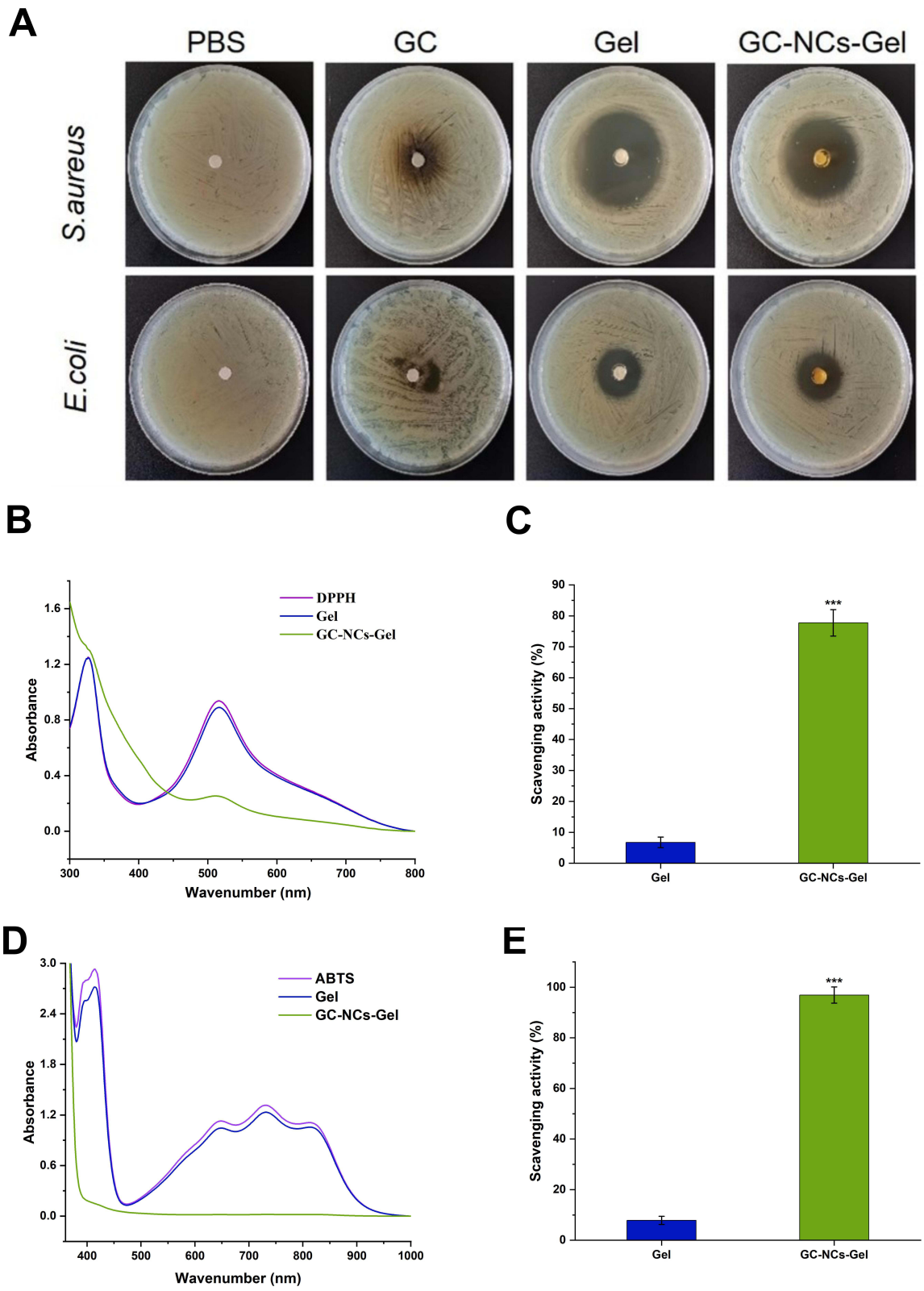

Figure 5 (**A**) Antimicrobial effects of GC, Gel, and GC-NCs-Gel. (**B**) Full-scan spectra by DPPH method. (**C**) Free radical scavenging of Gel and GC-NCs-Gel. (**D**) Full-scan spectra by ABTS method. (**E**) Free radical scavenging of Gel and GC-NCs-Gel. (****P* < *0.001*).

https://doi.org/10.2147/IJN.S514961

Specifically, for *S. aureus*, the diameters of inhibition zones of GC-NCs-Gel and Gel were 39.75 ± 0.61 mm and 42.38 ± 0.31 mm, respectively. For *E. coli*, they were 21.52 ± 0.06 mm and 21.30 ± 0.12 mm, respectively (Table 1). These results indicate that the prepared hydrogels have good antimicrobial effects and can provide an effective protective barrier for wounds against bacterial infection, thus promoting wound healing. Reactive oxygen species (ROS) play a dual role in the wound healing process, where an appropriate amount of ROS is essential for stimulating cell migration and angiogenesis, but an excessive amount of ROS can adversely affect wound healing.[47,48] To evaluate the antioxidant properties of the hydrogels, we tested them by DPPH and ABTS free radical scavenging experiments. The results of the DPPH free radical scavenging experiments (Figure 5B) showed that the absorbance at 517 nm decreased with the increase of the GC concentration in the hydrogel, indicating that the GC-NCs-Gel exhibited significant free radical scavenging ability after 30 min of incubation with scavenging efficiencies of up to 77.7% (Figure 5C).The results of the ABTS free radical scavenging assay (Figure 5D) showed that the absorbance at 516 nm decreased with increasing GC concentration, and the free radical scavenging efficiency of GC-NCs-Gel was up to 98.6% (Figure 5E). These results indicated that the incorporation of GC significantly enhanced the ROS scavenging ability of the hydrogel, which could be attributed to the abundant reduced phenolic groups in GC, which could act as electron donors and effectively neutralize free radicals. GC-NCs-Gel not only exhibited good antimicrobial activity, but also had excellent antioxidant properties, which makes it a promising drug delivery system.

Excision Wound Healing

Figure 6 shows that 24 h after constructing the rat whole-layer skin defect model, there was obvious oedema and a large number of inflammatory cells infiltration around the wounds in the experimental and model groups, and there was exudate around the wounds; on the 3rd day of drug administration, the oedema around the wounds in the experimental and model groups had been eliminated, and the wounds began to scab on the surface of the wounds. The wound area of the experimental group was reduced compared with that of the model group, and the wound healing rate of the model group was 16.2%, while that of the experimental group was 25.6%, which was improved compared with that of the model group. After 7 days of administration, the wound surface area of the experimental group decreased significantly, and the wound healing rate of the experimental group reached 68.3%, while the wound surface area of the model group had a small decrease relative to day 3, and the scab on the surface of the wound gradually hardened, and the inside of the flushed wound was accompanied by congestion; 15 days after the administration of GC-NCs-Gel, the model group showed an irregular shape of the scar, with black pigmentation, and the healing rate of the wound surface reached only 65.3%. In the experimental group, the wounds were almost healed, and the wound healing rate reached 95.3%, indicating

Table 1 Diameter of Inhibition Zone of GC, Gel and GC-NCs-Gel

Bacteria	Group	Inhibition Zone Diameter (mm)
E. coli	PBS	6.00
	GC	6.52±0.16**
	Gel	21.30±0.12***
	GC-NCs-Gel	21.52±0.06***
S. aureus	PBS	6.00
	GC	6.63±0.04^{ns}
	Gel	42.38±0.31***
	GC-NCs-Gel	39.75±0.61***

Notes: $^{ns}P>0.05$, $^{**}P < 0.01$,$^{***}P < 0.001$.

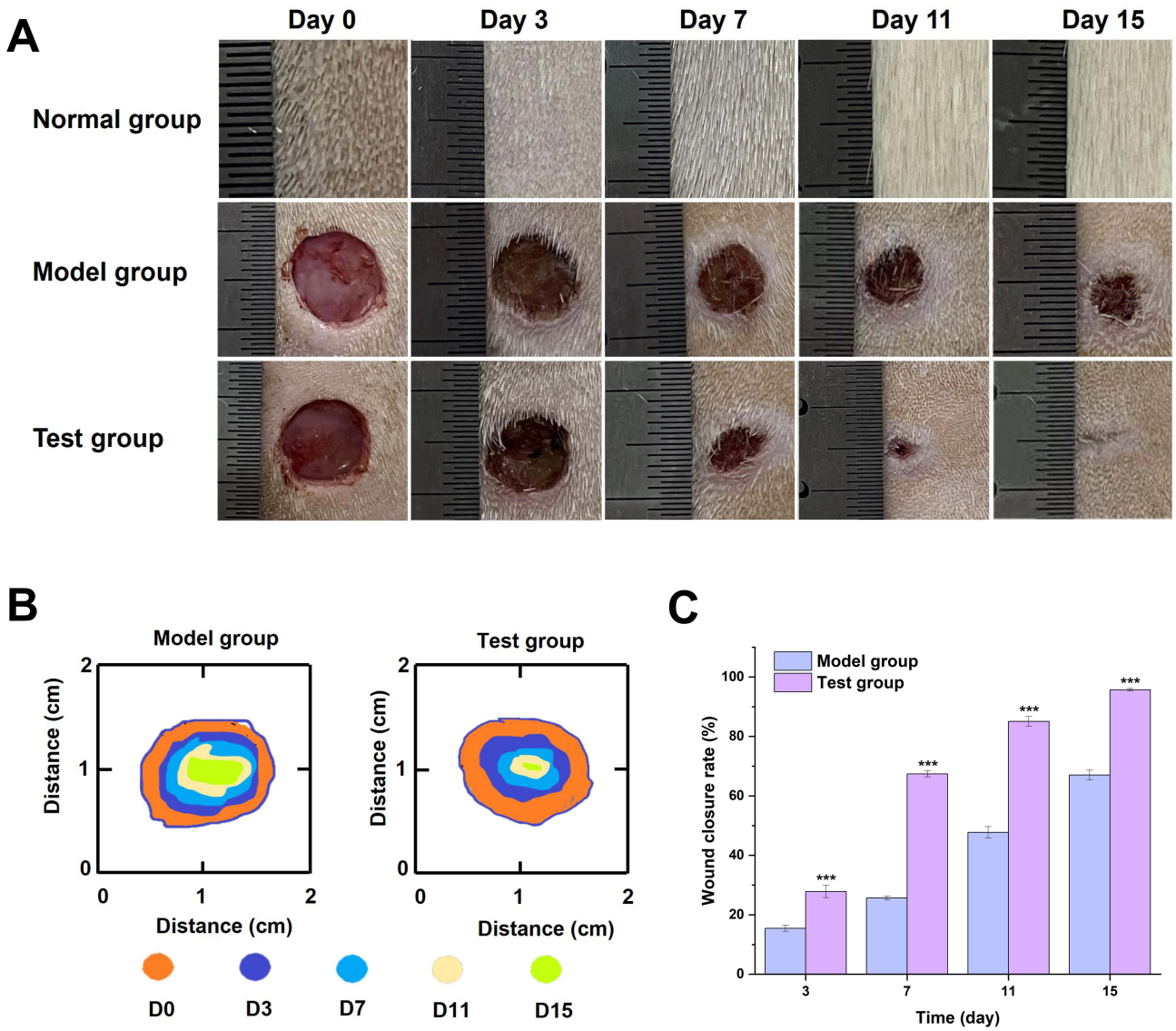

Figure 6 (**A**) Healing in different groups. (**B**) Fitting of wound healing traces on days 3, 7, 11 and 15. (**C**) Wound area remaining in rats after treatment in different groups. (***P < 0.001*).

that GC-NCs-Gel can promote wound healing and inhibit scar formation from anti-inflammatory, antibacterial and antioxidant aspects.

At the end of the experiment, paraffin embedding, slicing and H&E staining were performed on the skin tissue of the mice to observe the histopathological changes during wound healing. Histological results of the wounds on day 7 and day 15 (Figure 7A) showed. After 7 days of drug administration, both model and experimental groups were undergoing inflammatory response, the experimental group had more neovascularization as well as more lymphocyte infiltration in the wound, and the wound began to have epidermal production, indicating that the wound had begun to transform to the remodeling phase. The model group had fragments of necrotic cells as well as more lymphocytic infiltration. After 15 days of administration, the experimental group showed significant neovascularization, and the epidermis at the wound site formed a more complete and thickened structure than the control group (Figure 7B). In addition, a large number of skin appendages, including hair follicles and sebaceous glands, appeared in the dermis, and the formation of these appendages further demonstrated the remarkable results of skin regeneration and repair in the experimental group. A large number of lymphocytes and a small amount of neovascularization were seen in the tissue sections of the model

https://doi.org/10.2147/IJN.S514961

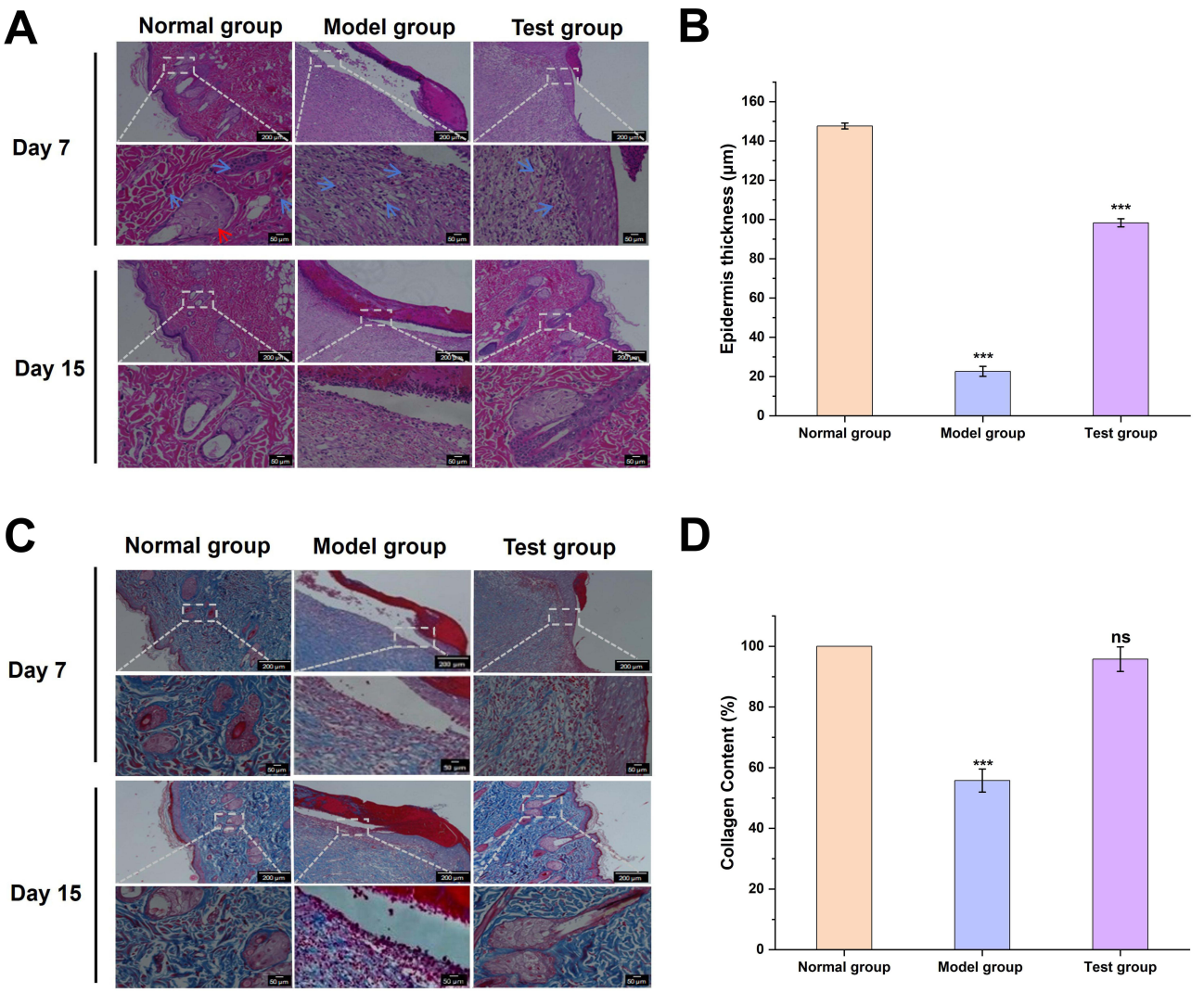

Figure 7 (**A**) H&E staining at skin wounds in different groups. (The blue and red arrows represent blood vessels and sebaceous glands, respectively) (**B**) Epidermal thickness. (**C**) Masson wound staining in different groups. (**D**) Collagen content (assuming 100% collagen content in normal group). (*$^{ns}P>0.05$, $^{***}P < 0.001$*).

group, indicating that the model group was still in the inflammatory phase. Taken together, these results suggest that GC-NCs-Gel can promote the transformation of cells from the inflammatory phase to the proliferative phase, thereby promoting wound healing and inhibiting scar formation. As collagen deposition is also an important indicator of the effectiveness of wound healing, the distribution and density of collagen fibers were assessed using Masson staining.[49] The results (Figure 7C and D) showed that a certain amount of collagen was produced at the wound site in both the model group and the experimental group after 7 days of administration, and the collagen content at the wound site in the experimental group was higher than that in the model group. After 15 days of administration, Masson staining results showed that more collagen precipitation appeared in the experimental group, and the wound collagen distribution in the experimental group was more orderly and uniform, and the wound healing was complete without scar formation, indicating that GC-NCs-Gel promoted the movement of fibroblasts, promoted wound healing and inhibited scar formation. In the model group, the collagen content of the wounds was reduced compared with that of the experimental group, and there was no epidermalization, and the wound formation was incomplete.

In this study, we explored the dual role of macrophages in inflammatory response and tissue repair. Pro-inflammatory macrophages (M1-type) release inflammatory cytokines, such as tumor necrosis factor-α (TNF-α), involved in the

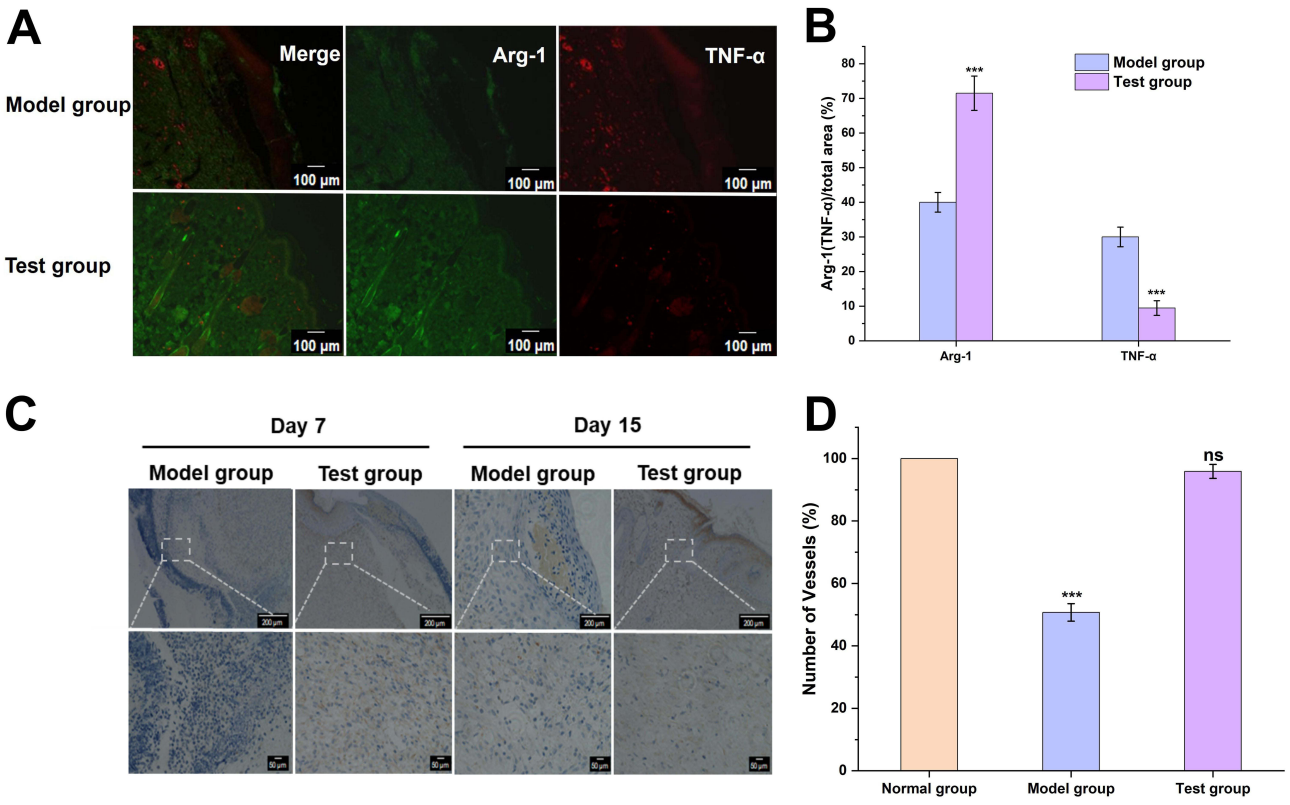

Figure 8 (**A**) Analysis of immunofluorescence results of TNF-α and Arg-1 inflammatory factors. (**B**) Analysis of quantitative results of immunofluorescence of TNF-α and Arg-1 inflammatory factors. (**C**) Immunohistochemistry of VEGF at the wounds of different groups. (**D**) Number of neovascularization at the wounds of different groups. (*$^{ns}P>0.05$, $^{***}P < 0.001$*).

initiation and maintenance of the inflammatory response to remove pathogens and damaged tissue.[50] In contrast, anti-inflammatory macrophages (M2) inhibit inflammation and promote tissue repair by secreting factors such as arginase-1 (Arg-1).[51] The experimental results showed that the expression of Arg-1 was significantly up-regulated and the expression of TNF-α was significantly down-regulated in the experimental group compared with the model group (Figure 8A and B), which indicated that GC-NCs-Gel was able to effectively inhibit inflammatory responses and promote tissue repair. GC-NCs-Gel reduced the degree of inflammation by inhibiting the secretion of inflammatory factors from the M1-type macrophage cells, creating a favorable wound healing environment for wound healing. In addition, the anti-inflammatory effect of GC-NCs-Gel facilitates the transition of the wound from the inflammatory phase to the proliferative phase, in which fibroblasts proliferate and synthesize extracellular matrix components, such as collagen, to fill in the wound defect, a key step in wound healing. Vascular endothelial growth factor (VEGF) is a key factor that promotes neovascularization.[52] We further investigated angiogenesis during wound healing and scar formation by immunohistochemical detection of VEGF. The results showed that the number of neovascularization in the GC-NCs-Gel group was significantly greater than that in the model group on the 7th day after administration (Figure 8C and D), suggesting that GC-NCs-Gel significantly promoted the formation of neovascularization. These new blood vessels provided essential nutrients and oxygen to the wound area, accelerating tissue repair and regeneration. By day 15 after administration, the wounds in the GC-NCs-Gel group had entered the remodeling stage and the neovascularization had begun to subside, whereas the wounds in the model group were still in the proliferative stage and the number of neovascularization was still high, further confirming the effectiveness of GC-NCs-Gel in accelerating wound healing.

Conclusion

In this study, we successfully prepared a novel nanogel, GC-NCs-Gel, a delivery system consisting of nanocrystals (GC-NCs) made of gallic acid (GC), a plant polyphenol, uniformly dispersed in a polyacrylic acid hydrogel matrix. The GC-

https://doi.org/10.2147/IJN.S514961

NCs-Gel exhibited a homogeneous and highly interconnected network structure, with good solubility, degradation, water vapor transmission rate, mechanical properties and adhesion. In addition, GC-NCs-Gel is capable of sustained controlled drug release and excellent in vitro permeability. The incorporation of GC-NCs significantly enhanced the antibacterial and antioxidant properties of GC-NCs-Gel. Further biocompatibility studies demonstrated that GC-NCs-Gel exhibited significant wound healing-promoting effects in a rat skin defect scarring model. The delivery system effectively promoted granulation tissue formation and collagen deposition by promoting epidermal regeneration, inducing neovascularization, increasing the expression of the anti-inflammatory factor Arg-1, and decreasing the production of the pro-inflammatory factor TNF-α, thereby accelerating the wound healing process. To sum up, these effects, GC-NCs-Gel not only improved wound healing efficiency, but also helped to inhibit scar formation. Overall, GC-NCs-Gel demonstrated unique multifaceted effects in promoting wound healing and inhibiting scar formation, providing an efficient drug delivery system for wound healing.

Abbreviations

GC, Gallic acid; GC-NCs, Gallic acid nanocrystals; GC-NCs-Gel, Gallic acid nanocrystal hydrogel; WVTR, water vapor transmission rate; SDS, sodium dodecyl sulphate; SEM, scanning electron microscopy; XRD, X-ray diffraction; FT-IR, fourier transform infrared spectroscopy; DSC, differential scanning calorimetry; DPPH, 1,1-diphenyl-2-trinitrophenylhydrazine; ABTS, 2,2′-azino-bis (3-ethylbenzothiazoline-6-sulfonic acid); *E. coli*, Escherichia coli; *S. aureus*; Staphylococcus aureus; ROS, Reactive oxygen species; TNF-α, tumor necrosis factor-α; Arg-1, arginase-1; VEGF, vascular endothelial growth factor.

Data Sharing Statement

The data that support the findings of this study are available from the corresponding author (Junfeng Ban) upon reasonable request.

Ethics Approval and Informed Consent

The study was approved by the Institutional Animal Care and Use Committee of Guangdong Pharmaceutical University (gdpulacspf2022237), which ensures that the procedures employed meet guidelines for the care and use of laboratory animals. Sprague-Dawley rats were used in the experiment. The Guangdong Medical Animal Experimental Center provided the animals. Pigskin was provided by the Guangdong Provincial Laboratory Animal Monitoring Institute, and its use is ethical (gdpulacspf2022237). Moreover, approval was received prior to beginning this research.

Consent for Publication

The authors declare that they have no known competing financial interests or personal relationships that could have appeared to influence the work reported in this paper.

Author Contributions

All authors made a significant contribution to the work reported, whether that is in the conception, study design, execution, acquisition of data, analysis and interpretation, or in all these areas; took part in drafting, revising or critically reviewing the article; gave final approval of the version to be published; have agreed on the journal to which the article has been submitted; and agree to be accountable for all aspects of the work.

Funding

This work has received financial support from the Guangdong Provincial Forestry Science and Technology Innovation Project (2022KJCX012) and the Guangdong Provincial Drug Administration Science and Technology Innovation Section Project (2021TDB40).

Disclosure

The authors declare that they have no conflicts of interest in this work.

References

1. Liu H, Ai R, Liu BZ, He L. Tea polyphenol nano-crosslinked dynamical hyaluronic acid-based hydrogel for diabetic wound healing. *Int J Biol Macromol*. 2024;282(Pt 1):136856. doi:10.1016/j.ijbiomac.2024.136856
2. Liu S, Zhao Y, Li M, et al. Bioactive wound dressing based on decellularized tendon and GelMA with incorporation of PDA-loaded asiaticoside nanoparticles for scarless wound healing. *Chem Eng J*. 2023;466:143016. doi:10.1016/j.cej.2023.143016
3. Almeleebia TM, Goyal N, Akhter MH, et al. *β*-cyclodextrin/PVP-stabilized nanocrystal gel for dual release of rutin and thymoquinone for wound healing. *J Clust Sci*. 2024;36(1):13. doi:10.1007/s10876-024-02735-5
4. Nayak M, Kumar V, Banerjee D, Pradhan L, Kamath P, Mukherjee S. Quercetin nanocrystal-loaded alginate hydrogel patch for wound healing applications. *J Mater Chem B*. 2025;13(5):1690–1703. doi:10.1039/D4TB01699H
5. Liang Y, He J, Guo B. Functional hydrogels as wound dressing to enhance wound healing. *ACS Nano*. 2021;15(8):12687–12722. doi:10.1021/acsnano.1c04206
6. Saboktakin MR, Tabatabaei RM. Supramolecular hydrogels as drug delivery systems. *Int J Biol Macromol*. 2015;75:426–436. doi:10.1016/j.ijbiomac.2015.02.006
7. Nuutila K, Eriksson E. Moist wound healing with commonly available dressings. *Adv Wound Care*. 2021;10(12):685–698. doi:10.1089/wound.2020.1232
8. Huang C, Dong L, Zhao B, et al. Anti-inflammatory hydrogel dressings and skin wound healing. *Clin Transl Med*. 2022;12(11):e1094. doi:10.1002/ctm2.1094
9. Zhang Q, Huang Z, Jiang H, et al. "Bamboo-like" strong and tough sodium alginate/polyacrylate hydrogel fiber with directional controlled release for wound healing promotion. *Carbohydr Polym*. 2025;347:122761. doi:10.1016/j.carbpol.2024.122761
10. Yang Z, Huang R, Zheng B, et al. Highly stretchable, adhesive, biocompatible, and antibacterial hydrogel dressings for wound healing. *Adv Sci*. 2021;8(8):2003627. doi:10.1002/advs.202003627
11. Zhang X, Wei P, Yang Z, et al. Current progress and outlook of nano-based hydrogel dressings for wound healing. *Pharmaceutics*. 2022;15(1):68. doi:10.3390/pharmaceutics15010068
12. Liu H, Chen L, Peng Y, et al. A tea polyphenol-loaded cellulose/silk fibroin/polyacrylic acid hydrogel for wound healing. *Cellulose*. 2024;31(13):8169–8187.
13. Shahrousvand M, Mirmasoudi SS, Pourmohammadi-Bejarpasi Z, et al. Polyacrylic acid/ polyvinylpyrrolidone hydrogel wound dressing containing zinc oxide nanoparticles promote wound healing in a rat model of excision injury. *Heliyon*. 2023;9(8):e19230. doi:10.1016/j.heliyon.2023.e19230
14. Sun X, Dong M, Guo Z, et al. Multifunctional chitosan-copper-gallic acid based antibacterial nanocomposite wound dressing. *Int J Biol Macromol*. 2021;167:10–22. doi:10.1016/j.ijbiomac.2020.11.153
15. Croitoru A, Ayran M, Altan E, et al. Development of gallic acid-loaded ethylcellulose fibers as a potential wound dressing material. *Int J Biol Macromol*. 2023;253:126996. doi:10.1016/j.ijbiomac.2023.126996
16. Yang DJ, Moh SH, Son DH, et al. Gallic acid promotes wound healing in normal and hyperglucidic conditions. *Molecules*. 2016;21(7):899. doi:10.3390/molecules21070899
17. Harwansh RK, Deshmukh R, Shukla VP, et al. Recent advancements in gallic acid-based drug delivery: applications, clinical trials, and future directions. *Pharmaceutics*. 2024;16(9):1202. doi:10.3390/pharmaceutics16091202
18. Kaparekar PS, Pathmanapan S, Anandasadagopan SK. Polymeric scaffold of gallic acid loaded chitosan nanoparticles infused with collagen-fibrin for wound dressing application. *Int J Biol Macromol*. 2020;165(Pt A):930–947. doi:10.1016/j.ijbiomac.2020.09.212
19. Gong W, Huang H, Wang X, He W, Hou Y, Hu J. Construction of a sustained-release hydrogel using gallic acid and lysozyme with antimicrobial properties for wound treatment. *Biomater Sci*. 2022;10(23):6836–6849. doi:10.1039/d2bm00658h
20. Mura PA, Cirri M, Rossetti A, Allemandi DA, Paredes AJ, Palma SD. Preparation of glyburide nanocrystals with improved dissolution properties by dry-ball- and wet-bead- milling: systematic comparison by experimental design of the performance of the two methods. *J Drug Deliv Sci Technol*. 2024;91:105222. doi:10.1016/j.jddst.2023.105222
21. Lin Y, Zhang Y, Cai X, et al. Design and self-assembly of peptide-copolymer conjugates into nanoparticle hydrogel for wound healing in diabetes. *Int J Nanomed*. 2024;19:2487–2506. doi:10.2147/IJN.S452915
22. Ma T, Yan L, Wang B, et al. Preparation and composition analysis of PVA/chitosan/PDA hybrid bioactive multifunctional hydrogel for wound dressing. *Eur Polym J*. 2024;221:113527. doi:10.1016/j.eurpolymj.2024.113527
23. Amini MA, Khodadadi I, Tavilani H, et al. Fabrication, characterization, and application of gelatin/alginate-based hydrogels incorporating selenium-doped deferoxamine-derived carbon quantum dots: in vitro and in vivo studies. *Int J Biol Macromol*. 2025;303:140569. doi:10.1016/j.ijbiomac.2025.140569
24. You M, Guo Y, Yu H, et al. Polyphenol-enhanced wet adhesive hydrogel with synergistic mechanical activation and ROS scavenging for accelerating diabetic wound healing. *Chem Eng J*. 2024;500:157103. doi:10.1016/j.cej.2024.157103
25. Zheng H, Wang J, Huang S, Xu X. Mechanically robust calcium alginate/polyacrylamide/tannic acid hydrogel with super toughness, adhesiveness and antimicrobial activity for pork freshness monitoring. *Int J Biol Macromol*. 2025;302:140539. doi:10.1016/j.ijbiomac.2025.140539
26. Hong R, Lai J, Mai D, Dai L, Lu Y, Lin J. Construction of chitosan/carboxylated polyvinyl alcohol/poly(n-isopropylacrylamide) composite antibacterial hydrogel for rapid wound healing. *Biomaterials Advances*. 2025;166:214041. doi:10.1016/j.bioadv.2024.214041
27. Moshfeghi T, Najmoddin N, Arkan E, Hosseinzadeh L. A multifunctional polyacrylonitrile fibers/alginate-based hydrogel loaded with chamomile extract and silver sulfadiazine for full-thickness wound healing. *Int J Biol Macromol*. 2024;279(Pt 4):135425. doi:10.1016/j.ijbiomac.2024.135425
28. Zhu F, Hu Y, Meng L, et al. Photo-crosslinking methacrylated-amylopectin/polyacrylamide hydrogels loading curcumin for applications as degradable, injectable, and antibacterial wound dressings. *Int J Biol Macromol*. 2024;278(Pt 3):134692. doi:10.1016/j.ijbiomac.2024.134692
29. Korolkovas A. Fast x-ray diffraction (XRD) tomography for enhanced identification of materials. *Sci Rep*. 2022;12(1):19097. doi:10.1038/s41598-022-23396-2

30. Chaudhary A, Kumar K, Singh VK, et al. Poly(acrylamide)-co-poly(hydroxyethyl)methacrylate-co-poly(cyclohexyl methacrylate) hydrogel platform for stability, storage and biocatalytic applications of urease. *Int J Biol Macromol*. 2024;265(Pt 2):131039. doi:10.1016/j.ijbiomac.2024.131039
31. Iijima M, Hatakeyama T, Hatakeyama H. DSC and TMA studies of polysaccharide physical hydrogels. *Anal Sci*. 2021;37(1):211–219. doi:10.2116/analsci.20SAR10
32. Zhang S, Gatsi B, Yao X, Jin Y, Amhal H. Cellulose nanofiber-reinforced antimicrobial and antioxidant multifunctional hydrogel with self-healing, adhesion for enhanced wound healing. *Carbohydr Polym*. 2025;352:123189. doi:10.1016/j.carbpol.2024.123189
33. Huang H, Yang X, Qin X, et al. Co-assembled supramolecular hydrogel of asiaticoside and panax notoginseng saponins for enhanced wound healing. *Eur J Pharm Biopharm*. 2025;207:114617. doi:10.1016/j.ejpb.2024.114617
34. Islam MM, Mondal MIH. Carboxymethyl cellulose/polyvinylpyrrolidone bio-composite hydrogels enriched with clove bud extracts for enhanced wound healing. *Arab J Chem*. 2024;17(9):105945. doi:10.1016/j.arabjc.2024.105945
35. Chen X, Yi L, Bai Y, et al. Antibacterial activity and mechanism of stevia extract against antibiotic-resistant Escherichia coli by interfering with the permeability of the cell wall and the membrane. *Front Microbiol*. 2024;15:1397906. doi:10.3389/fmicb.2024.1397906
36. Goyal R, Roy P, Jeevanandam P. Antibacterial activity studies of ZnO nanostructures with different morphologies against *E. coli* and *S. aureus*. *Appl Phys A*. 2023;129(4):244. doi:10.1007/s00339-023-06530-3
37. Allyn OQ, Kusumawati E, Nugroho RA. Antimicrobial activity of Terminalia catappa brown leaf extracts against staphylococcus aureus ATCC 25923 and pseudomonas aeruginosa ATCC 27853. *F1000Res*. 2018;7:1406. doi:10.12688/f1000research.15998.1
38. Gill SZ, Niazi MBK, Malik US, Jahan Z, Andleep S, Ahmed T. Development and characterization of SA/PEG hydrogel membranes with ag/ZnO nanoparticles for enhanced wound dressing. *Mater Chem Phys*. 2024;317:129170. doi:10.1016/j.matchemphys.2024.129170
39. Ouyang Y, Su X, Zheng X, et al. Mussel-inspired "all-in-one" sodium alginate/carboxymethyl chitosan hydrogel patch promotes healing of infected wound. *Int J Biol Macromol*. 2024;261(Pt 2):129828. doi:10.1016/j.ijbiomac.2024.129828
40. Liu H, Yang Y, Deng L, et al. Antibacterial and antioxidative hydrogel dressings based on tannic acid-gelatin/oxidized sodium alginate loaded with zinc oxide nanoparticles for promoting wound healing. *Int J Biol Macromol*. 2024;279(Pt 2):135177.
41. Zhou W, Yu Q, Ma J, Xu C, Wu D, Li C. Triamcinolone acetonide combined with 5-fluorouracil suppresses urethral scar fibroblasts autophagy and fibrosis by increasing mir-192-5p expression. *Am J Transl Res*. 2021;13(6):5956–5968.
42. Lin S, Quan G, Hou A, et al. Strategy for hypertrophic scar therapy: improved delivery of triamcinolone acetonide using mechanically robust tip-concentrated dissolving microneedle array. *J Control Release*. 2019;306:69–82. doi:10.1016/j.jconrel.2019.05.038
43. Jabeen N, Sohail M, Mahmood A, Ahmed Shah S, Mohammad Qalawlus AH, Khaliq T. Nanocrystals loaded collagen/alginate-based injectable hydrogels: a promising biomaterial for bioavailability improvement of hydrophobic drugs. *J Drug Deliv Sci Technol*. 2024;91:105291. doi:10.1016/j.jddst.2023.105291
44. Chen X, Wang X, Wang S, Zhang X, Yu J, Wang C. Mussel-inspired polydopamine-assisted bromelain immobilization onto electrospun fibrous membrane for potential application as wound dressing. *Mater Sci Eng C*. 2020;110:110624. doi:10.1016/j.msec.2019.110624
45. Bovone G, Dudaryeva OY, Marco-Dufort B, Tibbitt MW. Engineering hydrogel adhesion for biomedical applications via chemical design of the junction. *ACS Biomater Sci Eng*. 2021;7(9):4048–4076. doi:10.1021/acsbiomaterials.0c01677
46. Bakhtiari K, Kashanian S, Mohamadinooripoor R, Rashidi K, Sajadimajd S, Omidfar K. Synthesis and characterization of carboxymethyl chitosan/polyvinyl alcohol containing zinc oxide nanoparticles as hydrogel wound dressing. *Fiber Polym*. 2024;25(11):4199–4213. doi:10.1007/s12221-024-00748-5
47. Dong Y, Lv D, Zhao Z, Xu Z, Hu Z, Tang B. Lycorine inhibits hypertrophic scar formation by inducing ROS-mediated apoptosis. *Front Bioeng Biotechnol*. 2022;10:892015.
48. Huang F, Zhang E, Lei Y, Yan Q, Xue C. Tripterine inhibits proliferation and promotes apoptosis of keloid fibroblasts by targeting ROS/JNK signaling. *J Burn Care Res*. 2024;45(1):104–111. doi:10.1093/jbcr/irad106
49. Wang J, Zeng F, Pan N, et al. Umbilical cord mesenchymal stem cell exosomes combined with collagen sponges contribute to neovascularization and wound healing in exposed bone wounds. *Regenesis Repair Rehabilitation*. 2025;1(1):21–31. doi:10.1016/j.rerere.2024.09.002
50. Chen C, Amona FM, Chen J, et al. Multifunctional SEBS/AgNWs nanocomposite films with antimicrobial, antioxidant, and anti-inflammatory properties promote infected wound healing. *ACS Appl Mater Interfaces*. 2024;16(45):61751–61764. doi:10.1021/acsami.4c15649
51. Zhu W, Dong Y, Xu P, et al. A composite hydrogel containing resveratrol-laden nanoparticles and platelet-derived extracellular vesicles promotes wound healing in diabetic mice. *Acta Biomater*. 2022;154:212–230. doi:10.1016/j.actbio.2022.10.038
52. Chen X, Liu J, Lu Y, et al. A PLGA/silk fibroin nanofibre membrane loaded with natural flavonoid compounds extracted from green cocoons for wound healing. *Int J mol Sci*. 2024;25(17):9263. doi:10.3390/ijms25179263